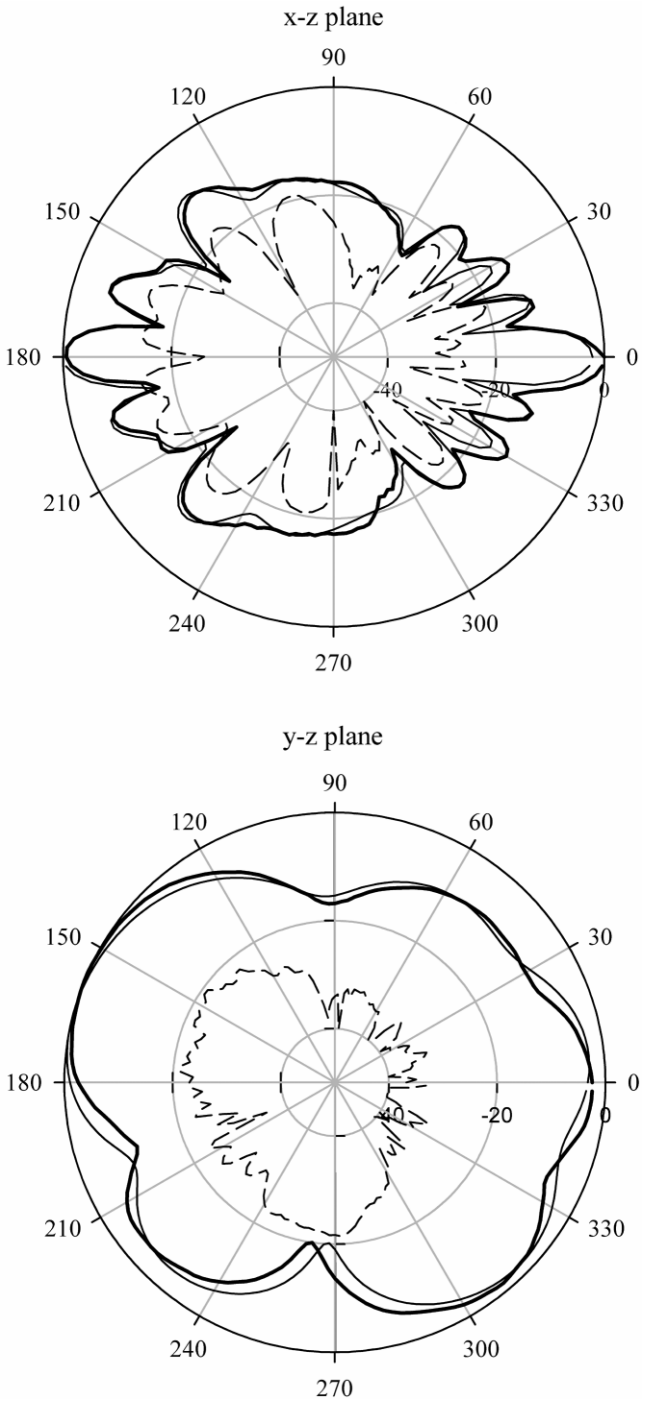


**Figure 10** Radiation pattern measurement versus simulation for (a) x–z plane and (b) y–z plane at 11 GHz for the 1 × 8 array, (▬▬: co-pol measured, - - - - : cross-pol measured, ——————: co-pol simulated)

configuration and compact size will be maintained. Simulations revealed that bi-directional radiation is eliminated and gain is apparently enhanced to around 15.5 dBi.

## 4. CONCLUSIONS

A novel microstrip array has been designed and experimentally characterized. The single element used to formulate the array is easily reconfigurable in terms of impedance bandwidth. Future implementations will be examined to simultaneously serve transmission and reception mode of modern satellite systems.


## ACKNOWLEDGMENT

The authors would like to thank Prof. Avaritsiotis and technician Mr. Koliopoulos for the prototype development. Additional credits to Taconic, for kindly providing the microwave dielectric laminates used for implementation of the antennas presented herein.


## REFERENCES


1. S.I. Latif, L. Shafai, and S.K. Sharma, Bandwidth enhancement and size reduction of microstrip slot antennas, IEEE Trans Antennas Propagat 53 (2005), 994–1003.
2. J.-Y. Sze and K.-L. Wong, Bandwidth enhancement of a microstrip-line-fed printed wide-slot antenna, IEEE Trans Antennas Propagat 49 (2001), 1020–1024.
3. Y.F. Liu, K.L. Lau, Q. Xue, and C.H. Chan, Experimental studies of printed wide-slot antenna for wide-band applications, IEEE Antennas Wireless Propagat Lett (2004), 273–275.
4. J. Powell and A. Chandrakasan, Differential and single ended elliptical antennas for 3.1–10.6 GHz ultra wideband communication, IEEE Antennas and Propagation Symposium, Monterey, CA, June 2004.
5. A.Z. Anastopoulos, E.S. Angelopoulos, D.I. Kaklamani, A. Alexandridis, F. Lazarakis, and K. Dangakis, Circular and elliptical CPW-fed slot and microstrip-fed antennas for ultra wide-band applications, Mediterranean Microwave Symposium, Athens, Greece, September 2005.


© 2006 Wiley Periodicals, Inc.

# SMALL PRINTED MEANDER SYMMETRICAL AND ASYMMETRICAL ANTENNA PERFORMANCES, INCLUDING THE RF CABLE EFFECT, IN THE 315 MHz FREQUENCY BAND


**Victor Rabinovich,[1] Basim Al-Khateeb,[2] Barbara Oakley,[3] and Nikolai Alexandrov[1]**

[1] Tenatronics Ltd., 776 Davis Drive, Newmarket, Ontario, Canada
[2] DaimlerChrysler Corporation, 800 Chrysler Drive Auburn Hills, Michigan
[3] Department of Electrical and Systems Engineering, Oakland University, Rochester, MI



*Received 17 February 2006*



**ABSTRACT:** *An easily manufactured, reduced size, symmetrical printed meander dipole antenna for remote keyless entry (RKE) automotive applications in the 315 MHz frequency band is proposed. The efficiency and directionality of this symmetrical antenna is estimated and compared with the efficiency and directionality of an asymmetrical antenna. Numerical and experimental results are presented.* © 2006 Wiley Periodicals, Inc. Microwave Opt Technol Lett 48: 1828–1833, 2006; Published online in Wiley InterScience (www.interscience.wiley.com). DOI 10.1002/mop.21790



**Key words:** *short-range communication; printed meander-line antenna; remote keyless entry system*


## 1. INTRODUCTION

In recent years, the wireless communication market has expanded greatly. Wireless devices such as remote control engine start systems, remote keyless entry (RKE) systems, and automatic tolling systems are now considered "classical " devices for short-range vehicle wireless communication [1–3]. Such control and security devices are commonly used in the 315 MHz frequency band in the United States, Canada, and Japan. In these systems, the antenna is a key element in determining system size and perfor-

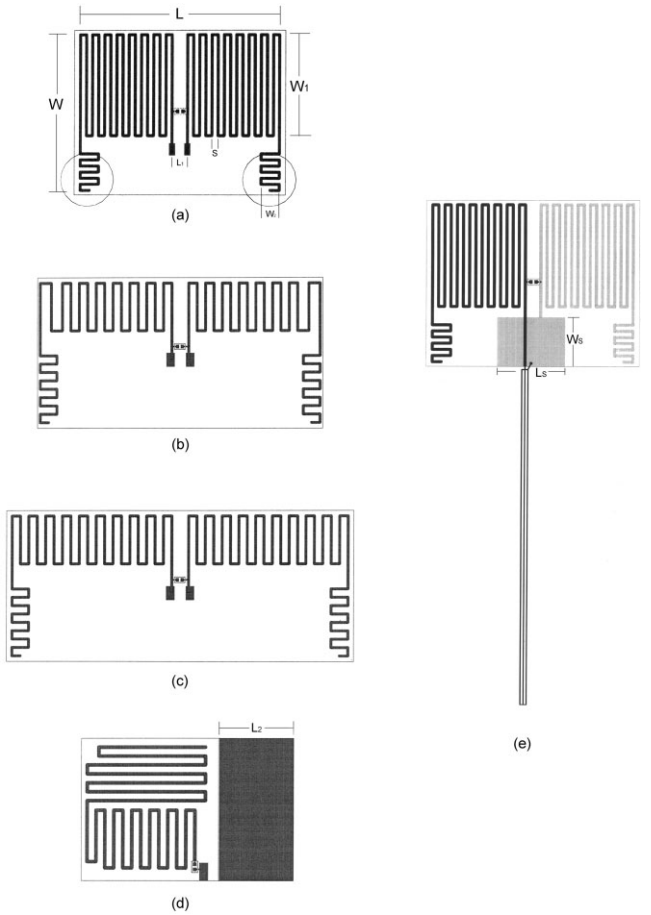


**Figure 1** Investigated antenna geometries: (a) $L = 70$, $L_1 = 5$, $W = 54$, $W_1 = 33$, $W_2 = 6$, $S = 1$; (b) $L = 100$, $L_1 = 6$, $W = 54$, $W_1 = 17$, $W_2 = 6$, $S = 3$; (c) $L = 120$, $L_1 = 6$, $W = 54$, $W_1 = 17$, $W_2 = 6$, $S = 3$; (d) $L = 70$, $L_2 = 24$, $W = 54$; and (e) $L = 70$, $L_1 = 5$, $L_s = 24$, $W = 54$, $W_1 = 33$, $W_2 = 6$, $W_s = 12$, $S = 1$

mance. Examples of external (that is, on the exterior of the vehicle) and internal antennas that are in current production are discussed in references [4–6]. Internal antennas as a rule are printed on dielectric boards together with electronic components of the RKE systems [4]. The integration of RF and digital electronic components with receiving antennas reduces the number of wires and connectors and therefore reduces the system cost. However, such designs have one significant disadvantage: parasitic emissions from electronic components (oscillators) located on the circuit board that can markedly reduce the communication range. An external dipole antenna [5] does not have such a disadvantage because it is isolated from the control electronics elements. Unfortunately, such antennas, with lengths of about 30 cm, are large and inconvenient for interior vehicle applications.

The "pigtail" coaxial antenna described in the patent of Ref. 6 avoids some of the problems seen in external dipoles, and is thus more convenient for automotive interior applications. The pigtail is made by simply stripping off the outer conductor of the coax to extend the inner conductor by a quarter-wavelength. The cable thus becomes a part of the antenna [7–9]. (Coaxial antenna parameters are detailed in Ref. 8.) The problem with the pigtail, however, is that in automotive applications pigtail antennas are positioned very close to the car body as a part of a cable harness. Because of the metal shadows from the car body, the pigtail has very small gain. The small gain in turn causes reduced communication range. Therefore, in applications where communication range is critical factor, pigtails are not acceptable for automotive antenna applications.

Planar meander antennas, as described in references [10–14], are small but highly efficient. Reference [14], for example, describes a small asymmetrical printed-on-FR4-dielectric external passive antenna and an active antenna for interior 315 MHz automotive applications. An important point related to asymmetrical antenna design such as that described in [15] is that there is significant current flow in the outer conductor of the RF cable that connects an antenna with RKE control module. Essentially, the cable becomes a part of the antenna and provides for extended range. A drawback of such asymmetry, however, is that the cable location influences the communication range of the RKE system. Modern vehicles have many different electronic devices, including heaters, air conditioning modules with automatic temperature control, audio amplifier systems, heated seat modules, power control modules, and sunroof modules. Parasitic emissions from the electronic devices near the routing path of the external antenna's RF cable can reduce the communication range of the asymmetric RKE system. In fact, EMC measurements show that such interference can exceed the noise floor level of the RKE system by more than 20 dB.

To gain a feel for how an RKE system can be affected by "real life" interference, let us assume that a nominal communication range for an asymmetric RKE system is 100 m in the absence of parasitic emissions. Experimental measurements show that the noise received by the RF cable can exceed the noise floor of the RKE by 20 dB. According to the simulation graphs shown in paper [16] such noise level reduces the communication range of the system to 20 m or less. Generally, the effect of parasitic components on a cable can be minimized by using a special balun [17]. Unfortunately, such a printed-on-circuit-board balun has a linear size equal to a quarter of the wavelength and therefore is too large for automotive for 315 MHz hidden applications. Therefore, automotive antenna designers are forced to use an antenna without a balun.

This article has two goals: first to investigate a symmetrical meandered dipole antenna with reduced linear size that appears to be a good candidate for 315 MHz automotive applications. This antenna could be used as a substitute for the asymmetrical antenna when interference becomes a problem for 315 MHz automotive antenna applications. Second, this paper numerically and experimentally estimates the effect of the RF cable (without a balun) on the parameters of both the symmetrical and asymmetrical antenna types. These investigations should be helpful in advancing the state of the art of interior vehicular antenna design.

**TABLE 1 Simulation Results of the Radiation Efficiency $\eta$ for Different Linear Antenna Sizes**

| | | Efficiency $\eta$ | |
|---|---|---|---|
| Type | Length (mm) | Without Cable | With 1 m Cable |
| Printed meandered dipole | 70 | 0.23 | 0.28 |
| | 100 | 0.42 | 0.45 |
| | 120 | 0.52 | 0.54 |
| | 70 + ground spot | 0.21 | 0.33 |
| Printed asymmetrical meander line | 70 | 0.12 | 0.45 |
| Wire half-wave dipole | 475 | 0.98 | 0.98 |

$f = 315$ MHz

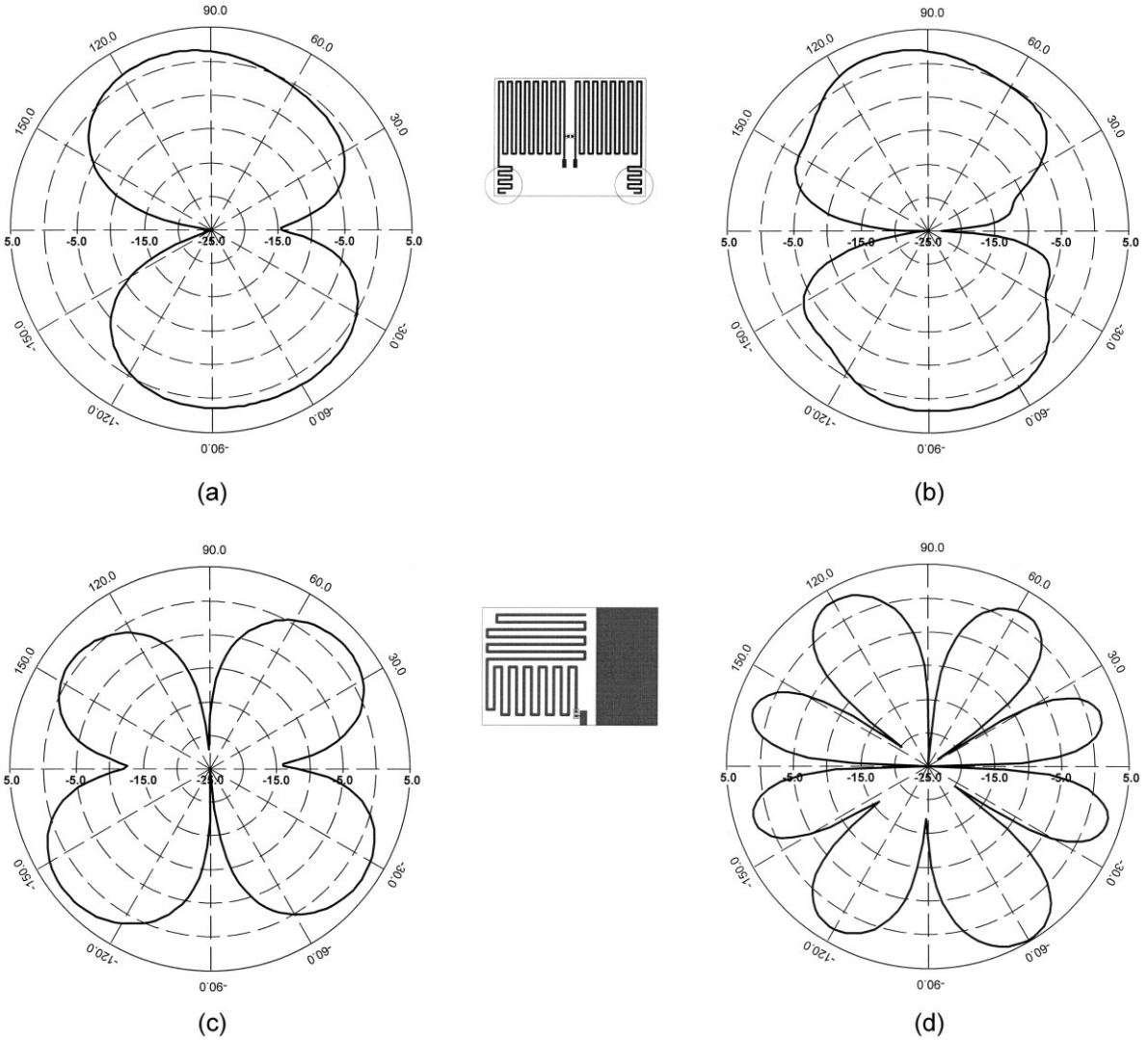


**Figure 2** Simulated results: (a) symmetrical meander line dipole, $L_c = 65$ cm; (b) symmetrical meander line dipole, $L_c = 160$ cm; (c) asymmetrical meander line antenna, length $L_c = 65$ cm; and (d) asymmetrical meander line antenna, $L_c = 160$ cm

## 2. ANTENNA GEOMETRY

Meander line antennas with several different lengths $L$ and widths $W$ are shown in Figure 1. All significant antenna geometry linear parameters shown in Figure 1 are presented in millimeters. The width of the printed antenna trace lines is 1 mm. Symmetrical dipole geometries have an increasing $L$ from Figures 1(a)–1(c), but all values of $L$ are still less than 1/10 wavelength. The asymmetrical meander line antenna [14] shown in Figure 1(d) has the same linear size in $L$ and $W$ as the antenna shown in Figure 1(a). The ratio $W/L$ for each antenna is less than 1. All antennas are printed on the FR4 substrate, with a thickness of 1.6 mm and a relative permittivity of 4.4. Antennas shown in Figures 1(a)–1(d) are printed on one side of the dielectric board, and the antenna presented in Figure 1(e) is a double-sided printed antenna. Black lines are drawn on the top of the dielectric, while grey lines together with a ground spot are located on the bottom side of the dielectric. The antennas presented in Figures 1(d) [10] and 1(e) have a spot that can be used as a ground for the amplifier circuit when using the antenna in an active receiving design. Figure 1(e) shows geometry of the assembly, including the antenna and the RF cable. The total printed line length and the number of bends for each antenna were chosen using the electromagnetic software package IE3D to provide 50 Ω input impedance. Accurate impedance tuning was achieved experimentally by insertion of an inductor between the positive and negative dipole arms and additional cutting of the edge meander antenna copper trace bends (these

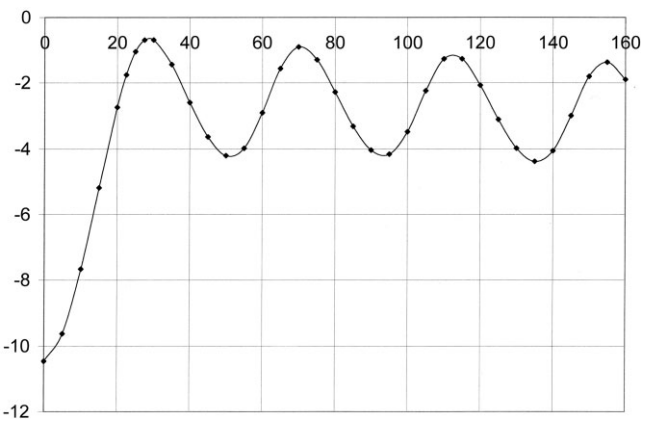


**Figure 3** Efficiency as a function of the cable length for asymmetrical meander line antenna

**TABLE 2 Calculated Results**

| Type | Length (mm) | Mean Square Error $\varepsilon$ |
|---|---|---|
| Printed meandered dipole | 70 | 0.3 |
| | 100 | 0.16 |
| | 120 | 0.15 |
| | 70 + ground spot | 0.74 |
| Printed asymmetrical meander line | 70 | 0.81 |

$f = 315$ MHz

antenna components are shown in Figure 1(a) by circles). The tuning of the meander asymmetrical antenna impedance to 50 Ω was provided by an additional capacitor inserted between the meander line and a ground spot close to the input antenna port. All antennas were operated as external antennas connected with a control RKE module through the RF cable.

### 3. NUMERICAL RESULTS

We investigated the radiation efficiency $\eta$ of each of the antennas that had been shown in Figure 1 through the use of IE3D electromagnetic software. The efficiency and the directionality were each calculated both with and without an RF cable. Table 1 presents the simulation results of the radiation efficiency $\eta$ for different linear antenna sizes.

As the table reveals, the meander asymmetrical antenna without an RF cable had the lowest antenna efficiency value: 0.12 (−9.2 dB). In comparison, the symmetrical meander dipole antenna was 1.9 times more efficient. But the table also reveals that the asymmetrical meander antenna (70 mm linear size) with an RF cable had the same efficiency as the 100 mm meandered dipole without an RF cable. This indicates that the cable had become a significant enhancement to the asymmetrical meander antenna. Such an antenna could therefore be effective in vehicle applications where electronic components near the RF cable do not radiate interference at the 315 MHz frequency band. It is significant to contrast these findings with those pertaining to the meandered dipole. In this latter instance, there is scarcely any difference between the efficiency of the antenna either with or without the RF cable. Naturally, this means that the RF cable effect for the symmetrical meandered antenna is minimal. (The presence of the small ground spot shown in Figure 1(e) does not appear to significantly influence the efficiency of the dipole.)

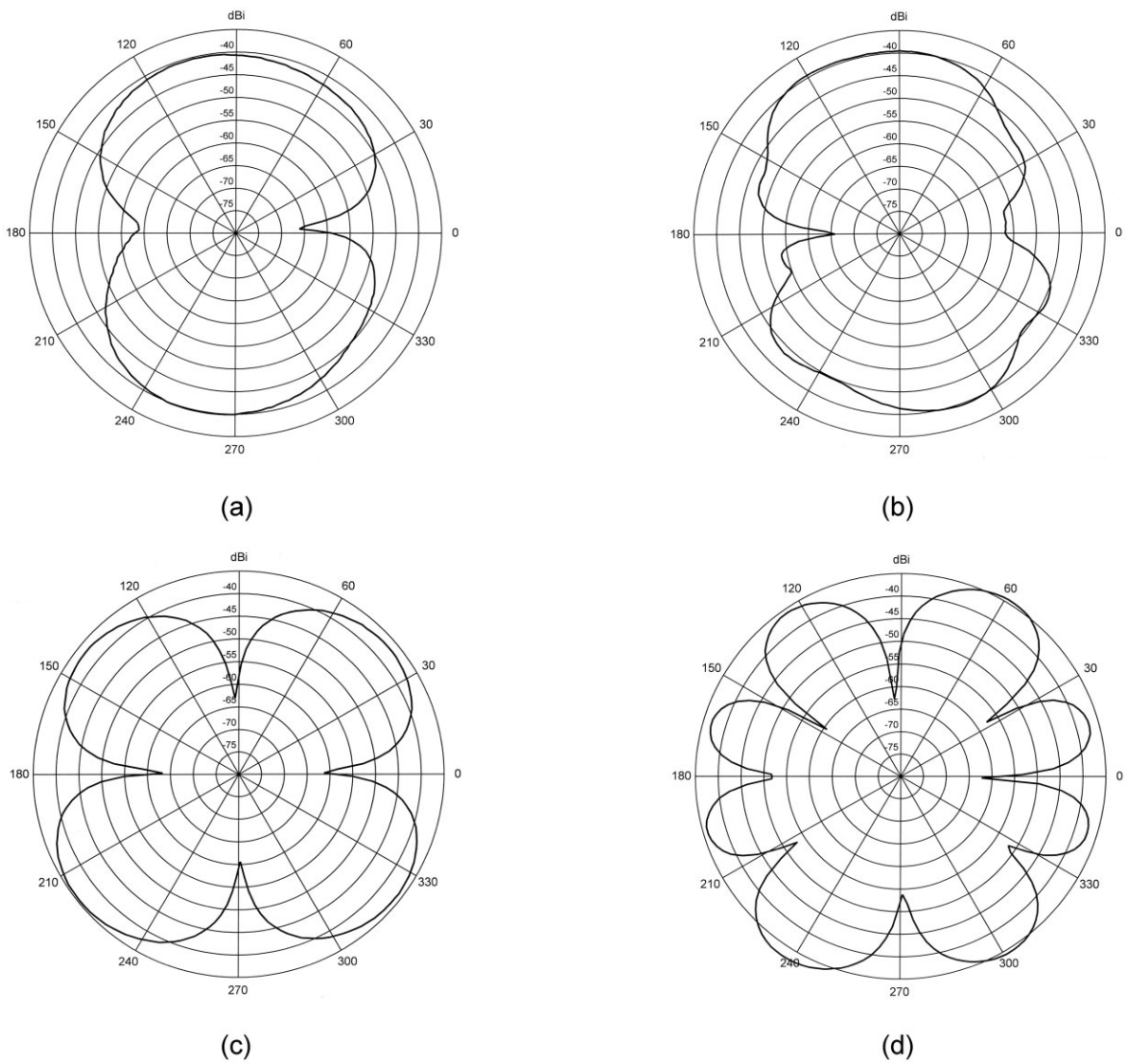


**Figure 4** Measurement results: (a) symmetrical meander line dipole, $L_c = 65$ cm; (b) symmetrical meander line dipole, $L_c = 160$ cm; (c) asymmetrical meander line antenna, $L_c = 65$ cm; and (d) asymmetrical meander line antenna, $L_c = 160$ cm

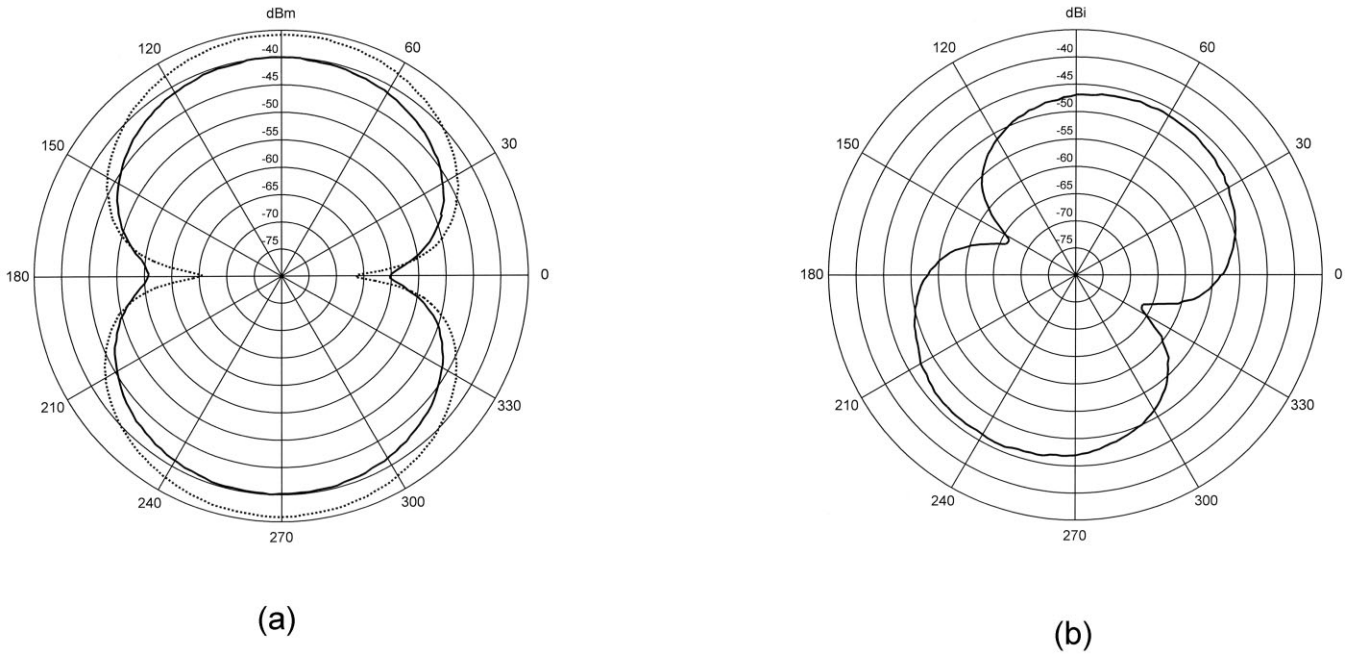


**Figure 5** Measurement results without RF cable: (a) solid line – symmetrical meander dipole, dotted line – reference antenna; (b) asymmetrical meander line antenna

More detailed numerical and experimental antenna directionality effects in the antenna plane were examined for both the symmetrical [Fig. 1(a)] and asymmetrical antennas [Fig. 1(d)]. Plots shown in Figures 2(a)–2(d) demonstrate calculated horizontally polarized directionalities with two different RG 174 RF cable lengths $L_c$. Antenna orientation with regard to the directionality angles is shown in Figure 2. It is seen that the asymmetrical antenna performances are similar to the performance of dipole antennas with total length values that cause a multi-lobe structure (that is, more than one wavelength).

Figure 3 shows the calculated ratio between the efficiency $\eta$ and cable length (expressed in centimeters) for the asymmetrical meander antenna shown in Figure 1(d). Efficiency expressed in dB format was normalized to the half-wave dipole efficiency. As can be seen, the asymmetrical antenna with the cable length around 25 cm has an efficiency almost equivalent to that of the half wave dipole. In such a configuration, the asymmetrical meander antenna together with its cable shows more gain than the symmetrical printed dipole. This efficiency is also very similar to that of a coaxial antenna with an inner conductor length value equal to one quarter of the wavelength, as described in [8]. Here, instead of the inner conductor of the coaxial antenna, we used a meander line with a linear size much less than one quarter wavelength but with a total trace length of more than a quarter wavelength.

We can introduce a mean square error parameter $\varepsilon$, averaged over 360°, which numerically estimates the "similarity" between two power directionality curves: the first when $F(\theta)$ corresponds to the antenna without a cable, and the second when $F_1(\theta)$ corresponds to the antenna with an RF cable,

$$\varepsilon = \frac{\int_0^{360} (F(\theta) - F_1(\theta))^2 \mathrm{d}\theta}{\int_0^{360} F^2(\theta) \mathrm{d}\theta}. \quad (1)$$

Table 2 shows the calculated results. As can be seen, the asymmetrical antenna has a maximum error value $\varepsilon$, which means that this antenna benefits from the largest increase in gain due to the added effect of the cable, but can suffer from interference effects due to parasitic interference sources in the car located close to the RF cable route. The meander symmetrical dipole has the smallest error $\varepsilon$, which means that this antenna has a minimal benefit from the addition of the cable, but also minimal possible interference effect. From these results, it is possible to conclude that, if a car does not have electronic components that radiate parasitic emissions at 315 MHz, it is preferable to use an asymmetrical antenna design with careful RF cable routing that can increase the communication range. However, if electronic components radiate parasitic emissions near the cable path route, a symmetrical dipole antenna is a better candidate for RKE automotive applications. Always, the first design step should be to investigate the noise environment in the car involving the RKE frequency band.

## 4. MEASUREMENT PROCEDURE

A passive meander line dipole antenna printed on an FR-4 dielectric substrate was placed horizontally (that is, the substrate board plane was parallel to the floor plane) on a turntable. The antenna was made to operate in the transmitting mode. A horizontally polarized receiving Yagi antenna operating in a frequency range from 300 to 1000 MHz was located in the far zone of the antenna assembly (this represented a passive antenna under test with an RF cable). Resulting directionality measurements are presented over 360° in the horizontal plane for the horizontal polarization. We used RG 174 cable for the measurements, with losses equal to 0.5 dB per meter in the 315 MHz frequency band.

## 5. MEASUREMENT RESULTS

The measurement results for the symmetrical and asymmetrical antennas shown in Figures 1(a) and 1(d) are presented in Figures 4 and 5. All plots shown in Figure 4 demonstrate the horizontal

polarization directionality graphs in the azimuth plane for an antenna assembly consisting of a meander line antenna with different RF cable lengths.

Figure 4(a) reveals the directionality of a symmetrical dipole in the case where the cable length was equal to 65 cm. Figure 4(b) corresponds to a cable length of 1.6 m.

Figures 4(c) and 4(d) show the horizontally polarized directionality plots in the azimuth plane for an antenna assembly consisting of an asymmetrical meander line antenna with an RF cable. Figures 4(c) and 4(d) show more than two main lobes. Again, we see good agreement between the simulated and measured results: both show very strong improvements on the antenna performances because of the effects of the cables.

Figures 5(a) and 5(b) reveals the antenna directionality of the meander dipole and asymmetrical meander line antenna ($L = 70$ mm) without an RF cable (the dashed line indicates the reference antenna directionality). The average (over 360°) gain of the printed dipole is less than the gain of the reference antenna by a value of $-4$ dB. The average gain of the asymmetrical meander line antenna is less than the gain of the reference antenna by a value of $-9$ dB. The measurement results confirm the findings of the numerical simulation: that the cable effect is not very significant in regards the performance of the symmetrical antenna. As can be shown the medium ($L = 100$ mm) and large antenna ($L = 120$ mm) sizes reveal the same level of agreement between simulation and measurement results.

### 6. CONCLUSIONS

We have presented a novel reduced-size printed symmetric meander dipole antenna design for use in the 315 MHz frequency band, and investigated its performance in comparison with related antennas. The antennas investigated here are less than 1/10 of the wavelength in size, possess high efficiency (not less than $-4$ dB) compared to a half wave dipole, are subject to minimum cable effect on the antenna performance, and therefore can be a good candidate as hidden antennas for automotive RKE applications. Increase of linear size of the antenna from 70 to 120 mm (as can be seen from Table 1) does not markedly increase the antenna gain or communication range. Numerical simulation of the RF cable effects on the antenna parameters show good agreement with experimental results.

### REFERENCES


1. A. Bensky, Short-range wireless communications, LLH Technology Publishing, 2000.
2. F.L. Dacus, Design of short-range radio systems, Microw RF 40 (2001), 73–80.
3. A.I. Alrabady and S.M. Mahmud, Analysis of attacks against the security of keyless-entry systems for vehicles and suggestions for improved designs, IEEE Trans Vehic Technol 54 (2005), 41–50.
4. L. Burr, F. Berg, T. Childs, J. Cerva, and S. Gillman, Column electronics control assembly, US Patent No. 6,731,020 B2 (2004).
5. H. Blaese, Inside window antenna, US Patent No. 5,027,128 (1991).
6. M. Wiedmann, M. Pfletschinger, and D. Wendt, Antenna for a central locking system of an automotive vehicle, US Patent No. 6,937,197 B2, (2005).
7. F. Hab, Radiated emission from shielded cables by pigtail effect, IEEE Trans Electromagn Compatibility 34 (1992), 345–348.
8. B. Drozd and W.T. Joines, Comparison of coaxial dipole antennas for applications in the near-field and far field regions, Microw J (2004).
9. S. Saaro, D.V. Thiel, J.W. Lu, and S.G. O" Keefe, An assessment of cable radiation effects on mobile communications antenna measurements, IEEE AP-S Int Symp Dig 1 (1997), 550–553.
10. M. Takiguchi and Y. Yamada, Radiation and ohmic resistances in very small meander line antennas of less than 0.1 wavelength, Electron Commun Jpn 88 (2005), 1–11.
11. M. Takiguchi and Y. Yamada, Input impedance increase of a very small meander line antenna, Proc IEEE AP-S Int Symp Dig 1 (2003), 856–859.
12. T. Endo, Y. Sunahara, S. Satoh, and T. Katagi, Resonant frequency and radiation efficiency of meander line antennas, Electron Commun Jpn 83 (2000), 52–58.
13. R. Azadegan and K. Sarabandi, A compact folded-dipole antenna for wireless applications, Proc IEEE AP-S Int Symp Dig 1 (2003), 439–442.
14. B. Al-Khateeb, V. Rabinovich, and B. Oakley, An active receiving.antenna for short-range wireless automotive communication, Microw Opt Technol Lett 44 (2004), 200–205.
15. O. Staub, J. Zurcher, and A. Skrivervic, Some considerations on the correct measurement of the gain and bandwidth of electrically small antennas, Microw Opt Technol Lett 17 (1998), 156–160.
16. V. Rabinovich, B. Al-Khateeb, B. Oakley, and N. Alexandrov, A signal and noise-measurement procedure for an antenna/RF receiver combination in a short-range automotive communication system, Microw Opt Technol Lett 47 (2005), 116–119.
17. K.V. Pugilia, Application notes: Electromagnetic simulation of some common balun structures, IEEE Microw Mag 3 (2002), 56–61.


© 2006 Wiley Periodicals, Inc.

## FIBER-OPTIC ACOUSTIC TRANSDUCER UTILIZING A DUAL-CORE COLLIMATOR COMBINED WITH A REFLECTIVE MICROMIRROR

**Ju-Han Song and Sang-Shin Lee**
Department of Electronic Engineering
Kwangwoon University, Nowon-Gu
Seoul 139–701, South Korea

*Received 17 February 2006*

**ABSTRACT:** *A photonic acoustic transducer utilizing a dual-core fiber collimator and a membrane type micromirror was proposed and demonstrated. The collimator and the mirror serve as a compact optical head and a reflective diaphragm, respectively. The micromirror diaphragm is suspended by a silicon bar connected to a frame, allowing for displacement induced by acoustic waves. The optical head incorporating dual collimators integrated in a single housing provides light to and receives it from the diaphragm. It facilitates the initial adjustment of the distance between it and the diaphragm, thanks to its slowly varying beam profiles. For the proposed acoustic transducer, the static characteristics were measured to find the operation point defined as the optimum distance between the head and the diaphragm, and a frequency response with a variation of ~±5 dB was achieved for the range of up to 3 kHz.* © 2006 Wiley Periodicals, Inc. Microwave Opt Technol Lett 48: 1833–1836, 2006; Published online in Wiley InterScience (www.interscience.wiley.com). DOI 10.1002/mop.21789

**Key words:** *acousto-optic sensor; acoustic wave; transducer; micromirror; fiber-optic component*

In recent years, a photonic acoustic transducer [1] has attracted immense amount of interests as a promising microphone because of its advantages over the conventional capacitive counterpart [2] like immunity to electromagnetic interference, smaller diaphragm size, less sensitivity to vibration, lighter weight, and higher directionality. Its applications include the patient-to-doctor communication in a magnetic resonance imaging system and a computed tomography (CT) system, the remote air-traffic monitoring under noisy circumstances, the vehicle identification, and the high performance speech recognition. Of the properties of light used for acousto-optic transducers, the intensity [3] is preferred to the phase